tvst

https://doi.org/10.1167/tvst.8.3.1

Article

Novel Development of Parafoveal Capillary Density Deviation Mapping using an Age-Group and Eccentricity Matched Normative OCT Angiography Database

Jorge S. Andrade Romo[1], Rachel E. Linderman[2], Alexander Pinhas[1,3], Joseph Carroll[2,4], Richard B. Rosen[1,5], and Toco Y. P. Chui[1,5]

[1] Ophthalmology, New York Eye and Ear Infirmary of Mount Sinai, New York, NY, USA
[2] Cell Biology, Neurobiology & Anatomy, Medical College of Wisconsin, Milwaukee, WI, USA
[3] Ophthalmology, State University of New York Downstate Medical Center, Brooklyn, NY, USA
[4] Ophthalmology & Visual Sciences, Medical College of Wisconsin, Milwaukee, WI, USA
[5] Icahn School of Medicine at Mount Sinai, New York, NY, USA

Correspondence: Toco Y. P. Chui, 310 E 14th St, 5th Floor, South Building, New York, NY 10003, USA. e-mail: ychui@nyee.edu

Received: 11 July 2018
Accepted: 22 January 2019
Published: 1 May 2019

Keywords: retina; aging; capillary density; deviation map; optical coherence tomography angiography

Citation: Andrade Romo JS, Linderman RE, Pinhas A, Carroll J, Rosen RB, Chui TYP. Novel development of parafoveal capillary density deviation mapping using an age-group and eccentricity matched normative OCT angiography database Trans Vis Sci Tech. 2019;8(3):1, https://doi.org/10.1167/tvst.8.3.1

Purpose: We evaluate the impact of age and signal strength index (SSI) on foveal avascular zone (FAZ) metrics and parafoveal capillary density measured using optical coherence tomography angiography (OCT-A), and propose a deviation mapping approach that accounts for age-group, SSI, eccentricity, and variation in FAZ size.

Methods: Parafoveal OCT-A with full vascular layer was obtained for 261 controls and four patients with retinal abnormalities. Parafoveal capillary densities were measured within eight consecutive 200-μm wide annuli from the FAZ border. In controls, the impacts of age and SSI on FAZ metrics and parafoveal capillary density were evaluated. Deviation maps highlighting regions with density at the lower and upper tails of the age-group and eccentricity matched distribution were generated.

Results: Linear regressions showed significant correlations between age, SSI, and mean parafoveal capillary density. There was a significant difference in FAZ metrics and parafoveal capillary densities with different age groups after controlling for SSI using univariate analysis. However, the effect of age on parafoveal capillary density disappeared after controlling for SSI using multivariate linear regression analysis. Our deviation mapping approach was able to identify regions with abnormal density in four patients.

Conclusions: Our findings suggest that the relationship between parafoveal capillary density and age is confounded by SSI. Parafoveal capillary density is SSI- and eccentricity-dependent. An age-group and eccentricity matched normative database was used as the basis for a parafoveal capillary density deviation mapping technique, providing an intuitive way to assess the status of parafoveal capillary density in individual eyes.

Translational Relevance: Understanding the impact of age and SSI on parafoveal capillary density is critical for providing accurate interpretation of OCT-A. We demonstrate an age-group and eccentricity matched deviation mapping technique for an intuitive assessment of retinal regions with abnormal density.

Introduction

Globally, the number of people 65 years or older is projected to increase from an estimated 524 million in 2010 to nearly 1.5 billion in 2050.[1] In the United States, the percentage of people 60 years or older is projected to increase from 22% in 2015 to 27% by the year 2050.[2] Ensuring that this population remains functional is critical for good quality of life, as well as minimizing the social and economic burdens of aging and age-related diseases on society.[3]

While various mechanisms of age-related tissue damage have been proposed, reduction of the overall homeostatic capacity to counteract oxidative stress, inflammation, and cellular damage appears most likely.[4–7] In the human eye, age-related accumulation of metabolic waste damages cells, resulting in reduced transparency of media, neural cell loss, and increased lipofuscin content.[8,9] These accumulations can contribute to cataracts, glaucoma, age-related macular degeneration, and diabetic retinopathy.[8,10,11] The retina is considered to be one of the most metabolically active tissues in the human body, and, thus, the retinal vasculature may be one of the earliest parts of the cardiovascular system to show age-related change.[12]

With aging, there is a varied degree of loss of capillary cellularity with endothelial cell degeneration.[9] There is a diminution in the number of capillaries around the fovea and also degeneration of smooth muscle arteriolar cells.[13] The result is decreased retinal blood flow, oxygen, and nutrition in the aging retina.[13] These alterations of retinal vasculature increase susceptibility to vision-threatening diseases, such as age-related macular degeneration and diabetic retinopathy, and may contribute to the development of glaucoma.[14]

Prior optical coherence tomography angiography (OCT-A) studies have suggested a decrease in parafoveal vessel density with age in otherwise healthy individuals.[15–17] However, the effect of age on parafoveal vessel density may have been confounded by the signal strength index (SSI). Reduced ocular media clarity in older participants resulting in lower SSI also leads to reduced parafoveal capillary density. Therefore, it is important to take consider this when judging the impact of aging on parafoveal capillary density. Many studies have used measurements of OCT-A vessel density, defined by percent area occupied by perfused vessels over total sampled area. Most methods used do not distinguish capillaries from noncapillary blood vessels. This approach may be problematic since capillary and noncapillary vessels have significant anatomic differences, lumen size dissimilarities, and separate roles in delivery of nutrition.

We evaluated the influence of age and SSI on parafoveal capillary density, using a method that excludes larger vessels and accounts for individual variations in foveal avascular zone (FAZ)[18] and retinal eccentricity.[19] We also introduced a novel deviation mapping approach that allows for a qualitative and quantitative assessment of the significance of regional parafoveal capillary density changes of an individual eye against a given age-group and eccentricity-matched normative data and illustrated the use of this approach in four eyes with retinal vascular abnormalities.

Methods

Study Population

This study was conducted at the New York Eye and Ear Infirmary of Mount Sinai and the Medical College of Wisconsin. The research protocol adhered to the tenets of the Declaration of Helsinki and was approved by the institutional review board of the New York Eye and Ear Infirmary of Mount Sinai and the Medical College of Wisconsin (PRO 23999). Written informed consent was obtained from all participants before imaging.

A total of 341 eyes of 341 healthy subjects were included in this study (69 recruited at the New York Eye and Ear infirmary of Mount Sinai and 272 at the Medical College of Wisconsin). Inclusion criteria were normal anterior segment, natural lens and clear media, and a self-reported negative past medical history with no known ocular or systemic disease. Exclusion criteria were nuclear, cortical, or posterior subcapsular cataracts $\geq$ grade 3 according to the Lens Opacity Classification System III,[20] other significant media opacities (i.e., corneal scarring, vitreous hemorrhage, anterior chamber inflammation), prior refractive surgery, and nystagmus or an inability to fixate. Only one eye from each subject was included for image processing and data analysis.[21] Four patients with nonproliferative diabetic retinopathy (NPDR), branch retinal vein occlusion (BRVO), sickle cell retinopathy (SCR), and oculocutaneous albinism were selected from a database of eyes with pathologies for demonstration of the parafoveal capillary density deviation mapping technique.

Image Acquisition

To confirm healthy eye status, fundus photographs (Zeiss Visucam; Carl Zeiss Meditec Inc., Dublin, CA) and OCT scans (Zeiss Cirrus HD-OCT; Carl Zeiss Meditec Inc., Dublin, CA; Heidelberg Spectralis HRA+OCT; Heidelberg Engineering, Inc., Heidelberg, Germany; Avanti RTVue-XR; Optovue, Fremont, CA) were acquired and reviewed on all healthy subjects. Subjects with the presence of any retinal vasculopathies or retinopathies were excluded. Features that identified as pathologic on fundus photo-

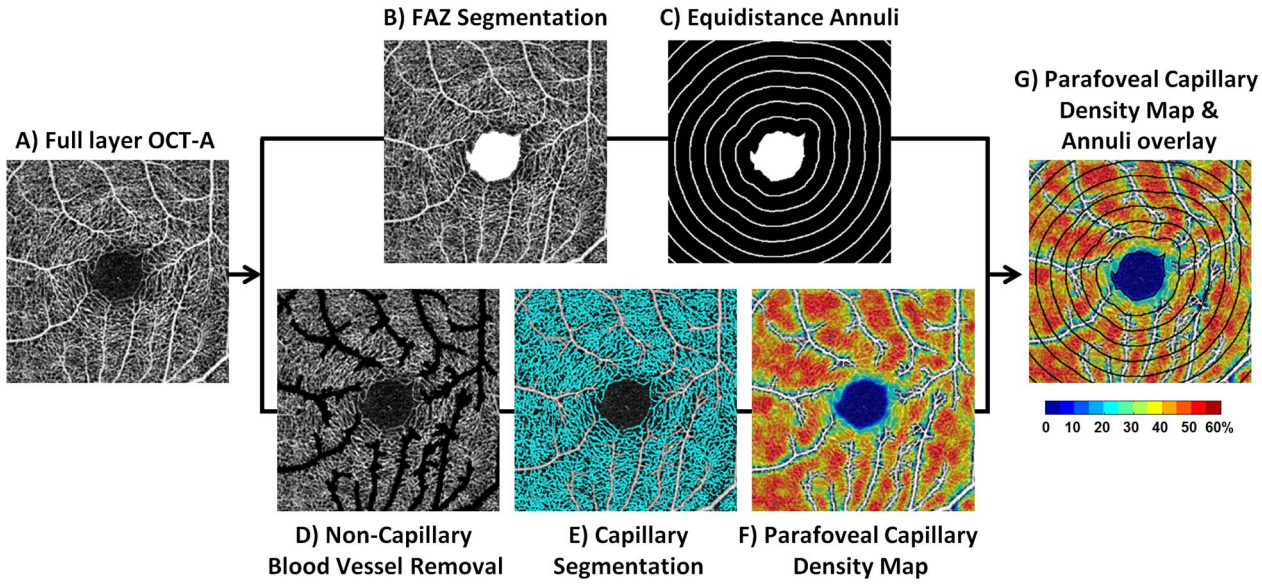

Figure 1. OCT-A image processing procedure. (A) Contrast-stretched full layer OCT-A. (B) Manual segmentation of FAZ border. (C) Creation of equidistant annuli with a 200 μm step size based on the FAZ border. (D) Removal of noncapillary blood vessels using global thresholding. (E) Segmentation of capillaries (in cyan) after removal of noncapillary blood vessels using local thresholding. (F) Parafoveal capillary density map. (G) Overlay of parafoveal capillary density map and equidistant annuli of increasing retinal distance from the FAZ border. On the parafoveal capillary density map, noncapillary blood vessels appear in white as they were excluded from the computation.

graphs or OCT scans were, but not limited to, hemorrhages, microaneurysms, occlusion of blood vessels, tortuous blood vessels, exudates, papilledema, macular edema, and retinal detachment. Dilated or undilated OCT-A macular scans were obtained with a commercial spectral domain OCT system (Avanti RTVue-XR; Optovue, Fremont, CA). Each OCT-A scan consisted of two volumetric 3 × 3 mm raster scans, one horizontal priority (x-fast) and one vertical priority (y-fast) B-scans. The Optovue OCT uses the split-spectrum amplitude-decorrelation angiography (SSADA) algorithm to generate OCT-A microvascular perfusion images of the retina.[22,23] SSI of each OCT-A was obtained. Axial length was measured in all eyes using the IOL Master (Carl Zeiss Meditec, Inc., Dublin, CA) and was used for retinal magnification correction on the OCT-A images.[24]

Image Processing

The imaging procedure used was similar to procedures previously published by our lab.[25] Using the AngioVue software (Optovue, versions 2016.2.0.16 and 2016.2.0.3), the full retinal vascular layer OCT-A containing capillaries and noncapillary blood vessels located between the inner limiting membrane and 70 μm below the posterior boundary of the inner plexiform layer was obtained from each eye Figure 1A. Then, each grayscale full layer OCT-A image (304 × 304 pixels) was resized by a factor of six (1824 × 1824 pixels; MATLAB 2013a; MathWorks, Natick, MA). The resized OCT-A image was contrast stretched by using the lowest and highest 1% pixel intensity values as the lower and upper intensity limits, respectively. On the contrast-stretched full layer OCT-A image, an FAZ mask was created by manually delineating the FAZ border using Adobe Photoshop (Adobe Systems, Inc., San Jose, CA; Fig. 1B). FAZ area, perimeter, and acircularity index were computed based on the FAZ mask as previously described.[25] We then compared parafoveal capillary density across eyes as a function of distance from the border of the FAZ by creating eight consecutive equidistant annuli from the FAZ border each 200 μm wide (Fig. 1C). The innermost annulus included the region of interest (ROI) from the FAZ border (0 μm) outward to 200 μm from the FAZ border. The outermost annulus represented ROI from 1400 to 1600 μm from the FAZ border. On the full layer OCT-A, noncapillary blood vessels were identified by replacing all pixel intensity greater than 0.7 with the value 1 (white) and the remaining pixels with the value 0 (black) using global thresholding. This binary mask then was used for removal of the pixels associated with the noncapillary blood vessels on the full layer OCT-A (Fig. 1D). Local thresholding then was performed for the segmentation of parafoveal per-

fused capillaries as described previously (Fig. 1E).[25] For qualitative assessment, a color-coded parafoveal capillary density map was created (Fig. 1F).

For quantitative assessment, parafoveal capillary density (%) was computed for each annulus (Fig. 1G) then was computed as described below:

$$\textit{Parafoveal capillary density}, \% = \frac{\textit{Parafoveal capillary area}}{\textit{Annulus area} - \textit{non-capillary blood vessel area}} \times 100\%$$

Visualization and Identification of Abnormal Parafoveal Capillary Density Regions using Deviation Mapping

For each age group, a normative database of parafoveal capillary density mean ± standard deviation (SD) was computed for the eight individual consecutive annuli and the ROI within the FAZ border. For purposes of demonstration, parafoveal capillary density deviation maps were generated for a control subject and four patients with retinal abnormalities (NPDR, BRVO, SCR, and albinism). For each tested eye, individual density value on the parafoveal capillary density map was first compared against the age-group–matched and eccentricity-matched normative database. Deviation map then was generated by highlighting the regions with a capillary density value below and above the normative database. On the deviation map, warmer colors indicated regions with parafoveal capillary density below 5% and 1% of the normal distribution, and cooler colors indicated regions with density above 95% and 99% of the normal population.

Statistical Analysis

SSI, FAZ metrics, and parafoveal capillary densities measured at different annuli in each age group were all tested for homogeneity of variance and normality using Levene's test and the Kolmogorov-Smirnov test, respectively. Correlations between age, SSI, and mean parafoveal capillary density were evaluated using linear regression (Pearson correlation coefficients, 2-tailed). One-way analysis of variance (ANOVA) with Bonferroni post hoc test was performed to evaluate the impact of age group on SSI. Univariate analysis then was performed to examine the impact of age group (as fixed factor, categorical independent variable) on FAZ metrics, and parafoveal capillary density measured at eight annuli (as continuous dependent variables) after controlling for SSI (as covariate, continuous variable). Multivariate linear regression analysis was performed using age and SSI (both as covariates, continuous variables) on FAZ metrics and parafoveal capillary density measured at eight annuli. Two-way ANOVA was performed to test for significance in the main effects and the interaction between age group and annular distance on parafoveal capillary density. All statistical analyses were performed using SPSS Statistics 24 (IBM Analytics, IBM Corporation, Armon, NY).

Results

We examined 341 healthy control eyes, 80 subjects were excluded due to poor image quality with the presence of blood vessel doubling, blinking artifact, or eye movement ($n = 32$), lack of complete data ($n = 32$), or health concerns ($n = 16$), 261 were deemed eligible healthy (148 female and 113 male; mean age, 37 years; age range, 5–87 years). Subjects were divided into seven groups according to age: ≤19, 20 to 29, 30 to 39, 40 to 49, 50 to 59, 60 to 69, and ≥70 years. The majority of the data showed equal variance and were normally distributed. Linear regressions and correlation coefficients of age, SSI, and mean parafoveal capillary density are shown in Figure 2. Linear regressions showed significant correlations between age, SSI, and mean parafoveal capillary density. SSI was significantly lower in the two oldest age groups (60–69 and ≥70) compared to other age groups (one-way ANOVA, Bonferroni post hoc test, $P < 0.05$). Demographic data for healthy subjects is displayed in Table 1. SSI and axial length measurements are displayed in Supplementary Tables S1 and S2.

FAZ Metrics Variation with Age Group

Boxplots of FAZ area, perimeter, and acircularity index are shown in Figure 3. The mean ± SD of FAZ area, perimeter, and acircularity index across all 261 healthy control subjects was 0.25 ± 0.10 mm^2, 2.23 ± 0.51 mm, and 1.30 ± 0.16, respectively. When analyzing all seven age groups, there were significant differences in FAZ area ($R^2 = 0.06$, $P = 0.022$), perimeter ($R^2 = 0.10$, $P = 0.0001$), and acircularity index ($R^2 = 0.14$, $P = 0.0001$) measured at each annulus after controlling for SSI using univariate analysis (Table 2). When analyzing all 261 subjects together as a single group, the effect of age (in years) on FAZ perimeter ($R^2 = 0.03$, $P = 0.009$) and acircularity index ($R^2 = 0.05$; $P = 0.0002$) remained significant after controlling for SSI using multivariate linear regression analysis (Table 2). However, no

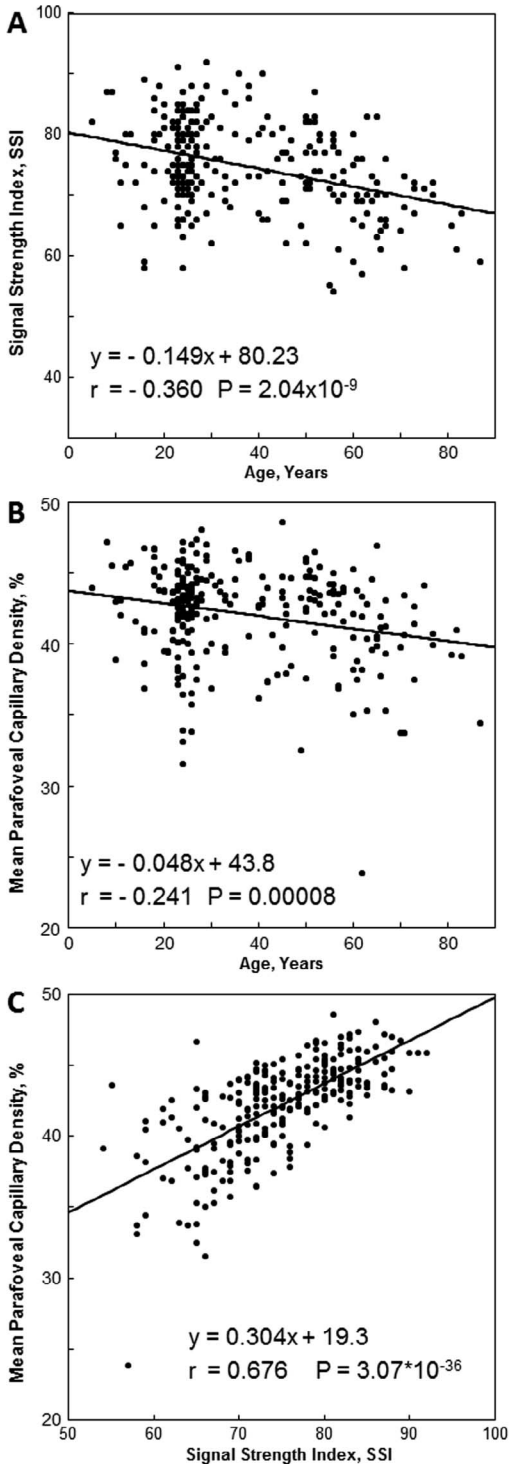

Figure 2. Linear regressions of (A) SSI and age, (B) mean parafoveal capillary density and age, and (C) mean parafoveal capillary density and SSI. Whereas mean parafoveal capillary density and SSI decreased with increasing age, mean parafoveal capillary density increased with increasing SSI.

Table 1. Demographic Data of All Age Groups

Age Group	No. of Subjects	Female/ Male	Mean Age (SD), Years
≤19	25	17/8	14 (4)
20–29	113	55/58	25 (2)
30–39	20	12/8	34 (3)
40–49	24	14/10	44 (3)
50–59	36	23/13	54 (3)
60–69	28	22/6	63 (3)
≥70	15	5/10	76 (5)
All subjects	261	148/113	37 (18)

significant effect of age on FAZ area was observed ($R^2 = 0.004$, $P = 0.545$).

Parafoveal Capillary Density Variation with Age Group at each Annulus

When analyzing all seven age groups, there was a significant difference in parafoveal capillary density measured at annulus 200 to 1200 μm with different age groups after controlling for SSI using univariate analysis ($R^2 = 0.30$–0.47, $P = 0.001$–0.05; Table 2). The youngest age group showed the highest mean density combining all annuli (43.6% ± 4.2%), while the oldest age group showed the lowest mean density (40.2% ± 3.0%; Table 3). When analyzing all 261 subjects together as a single group, however, the effect of age (in years) on all parafoveal capillary density measurements disappeared after controlling for SSI using multivariate linear regression analysis ($R^2 = 0.24$–0.44; $P = 0.077$–0.907; Table 2).

Parafoveal Capillary Density Variation with Age Group and Annular Distance

Significant main effects on parafoveal capillary density were found among age groups (2-way ANOVA, $P = 3.5 \times 10^{-44}$) and annular distances (2-way ANOVA, $P = 3.4 \times 10^{-176}$). Boxplots of parafoveal capillary density measured at increasing age group and annular distance are shown in Figure 4. In comparing parafoveal capillary density across age groups using Bonferroni post hoc tests, the oldest age group showed significantly lower density than the other five age groups (all $P < 0.0001$). Parafoveal capillary density increased with increasing annular eccentricity from the FAZ border with the lowest density measured at the 200 μm annulus (34.8% ± 3.9%), plateauing at the 800 μm annulus (44.1% ± 3.3%). In comparing parafoveal capillary density

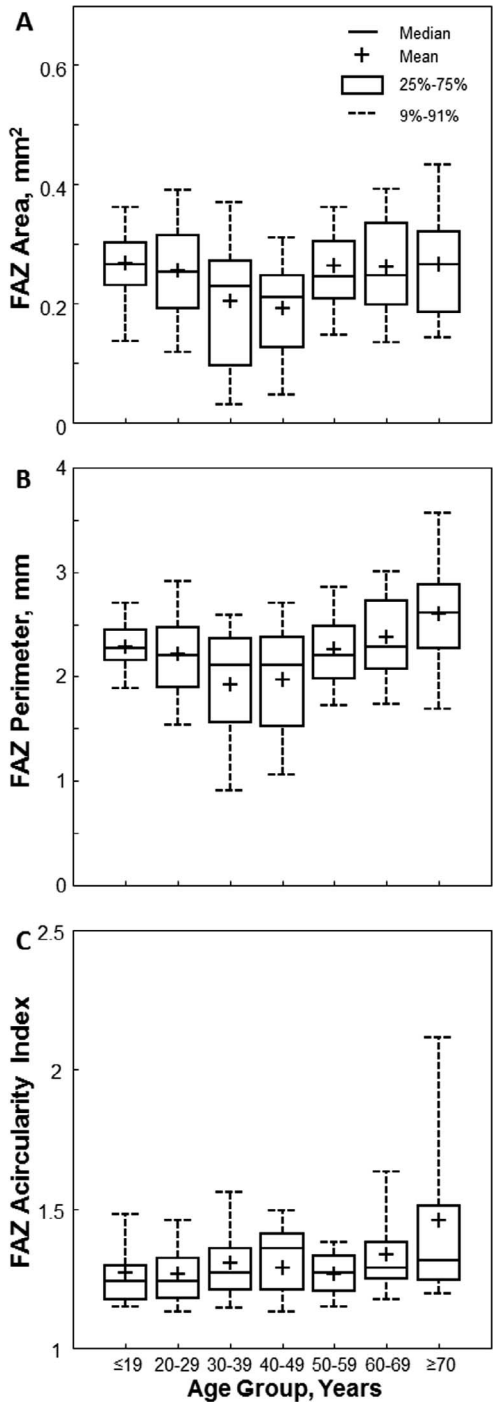

Figure 3. Boxplots of FAZ metrics in different age groups. (A) FAZ area. (B) FAZ perimeter. (C) FAZ acircularity index. Significant effect of age (in years) on FAZ perimeter and acircularity index was observed after controlling for SSI (multivariate linear regression analysis, $P = 0.009$ and $P = 0.0002$). No significant effect of age (in years) on FAZ area was observed (multivariate linear regression analysis, $P = 0.545$).

across annular distances using Bonferroni post hoc tests, 200 μm annulus showed significantly lower density compared to that in the other seven annuli (2-way ANOVA, Bonferroni post hoc tests, all P values <0.0001). Similar results were found at 400 μm annulus (2-way ANOVA, Bonferroni post hoc tests, all $P < 0.01$) except that no significant difference was found when compared to the 1600 μm annulus (2-way ANOVA, Bonferroni post hoc test, $P = 1.00$). No significant interaction between age group and annular distance was observed (2-way ANOVA, $P = 0.592$).

Deviation Mapping in Patients With Retinal Abnormalities

Figure 5 shows the visualization and identification of abnormal parafoveal capillary density regions on the five eyes included for demonstration, using the age-group–matched and eccentricity-matched deviation mapping technique. Deviation mapping identified diffuse regions with above normal density in the healthy controls (Fig. 5A), a focal subnormal perfusion defect in the NPDR eye (Fig. 5B), a subnormal perfusion defect in the superior retina of the BRVO eye (Fig. 5C), a diffuse subnormal perfusion defect in the SCR eye (Fig. 5D), and diffuse above normal density regions in the albinism eye (Fig. 5E).

Discussion

Our results demonstrated that there is a statistically significant difference in FAZ metrics between different age groups after controlling for SSI. While this result agrees with some previous studies,[26,27] others have found no significant correlation.[18,19] There are considerable challenges to address when analyzing FAZ, one being the high individual variation in the normal population.[28–31] Caution must be taken when comparing our results to previous studies, as unlike some studies, we corrected for retinal magnification based on individual axial length. Correction of retinal magnification based on axial length has been shown to impact FAZ and retinal vessel density measurements. Prior OCT-A studies have shown significant measurement errors of 30% to 50% in FAZ area and foveal vessel density without retinal magnification correction, thus, reducing their accuracy and reliability as biomarkers for disease detection and diagnosis.[19,24]

In agreement with most previous OCT-A studies, our results indicated that parafoveal capillary density

Table 2. Univariate Analysis and Multivariate Linear Regression Analysis Between Dependent Variables (FAZ Metrics and Parafoveal Capillary Densities) and Independent Variables (Age Group, Age, and SSI)

	Univariate Analysis			Multivariate Linear Regression		
DV	IV	R^2	*P* value	Covariate	R^2	*P* Value
FAZ metrics						
Area	Age group	0.06	0.022*	Age in year	0.005	0.545
	SSI		0.173	SSI		0.258
Perimeter	Age group	0.10	0.0001*	Age in year	0.03	0.009*
	SSI		0.037*	SSI		0.133
Acircularity index	Age group	0.14	0.0001*	Age in year	0.05	0.0002*
	SSI		0.144	SSI		0.330
Parafoveal capillary density						
Annulus 200 μm	Age group	0.30	0.001*	Age in year	0.24	0.378
	SSI		9.9×10^{-17}*	SSI		3.9×10^{-16}*
Annulus 400 μm	Age group	0.34	0.05*	Age in year	0.31	0.736
	SSI		7.8×10^{-19}*	SSI		6.8×10^{-20}*
Annulus 600 μm	Age group	0.38	0.031*	Age in year	0.35	0.077
	SSI		7.5×10^{-20}*	SSI		4.6×10^{-21}*
Annulus 800 μm	Age group	0.44	0.016*	Age in year	0.40	0.335
	SSI		7.6×10^{-25}*	SSI		2.6×10^{-26}*
Annulus 1000 μm	Age group	0.44	0.028*	Age in year	0.41	0.907
	SSI		1.3×10^{-26}*	SSI		4.4×10^{-28}*
Annulus 1200 μm	Age group	0.47	0.028*	Age in year	0.44	0.294
	SSI		4.6×10^{-30}*	SSI		3.8×10^{-32}*
Annulus 1400 μm	Age group	0.47	0.133	Age in year	0.44	0.856
	SSI		8.9×10^{-30}*	SSI		1.2×10^{-31}*
Annulus 1600 μm	Age group	0.45	0.098	Age in year	0.43	0.576
	SSI		4.1×10^{-28}*	SSI		1.2×10^{-30}*

In univariate analysis, parafoveal capillary densities measured at all eight annuli varied significantly with age group after controlling for SSI. The effect of age (in years) on all parafoveal capillary density measurements disappeared after controlling for SSI using multivariate linear regression analysis. DV, dependent variable; IV, independent variable; R^2, coefficient of determination.

* $P < 0.05$.

Table 3. Mean ± SD of Parafoveal Capillary Density Measured at Each Annulus in All Age Groups

	Parafoveal Capillary Density (±SD), %								
	Annulus								Mean 200–1600 μm
Age Group	200 μm	400 μm	600 μm	800 μm	1000 μm	1200 μm	1400 μm	1600 μm	
≤19	36.8 (3.9)	43.1 (2.1)	45.3 (2.1)	45.7 (2.5)	45.3 (2.9)	44.5 (3.4)	44.4 (3.8)	43.3 (4.8)	43.6 (4.2)
20-29	34.9 (3.5)	41.9 (2.7)	44.1 (2.5)	44.2 (3.0)	43.8 (3.6)	43.4 (3.7)	43.1 (3.9)	42.7 (4.2)	42.3 (4.5)
30-39	33.4 (4.5)	41.9 (2.4)	44.4 (2.3)	45.4 (2.0)	45.3 (2.5)	45.1 (2.9)	44.9 (3.8)	45.0 (3.9)	43.2 (4.9)
40-49	33.1 (3.9)	41.1 (3.3)	43.0 (3.1)	43.3 (3.2)	43.0 (3.7)	42.8 (4.1)	42.2 (4.8)	42.1 (4.7)	41.3 (5.0)
50-59	35.8 (3.2)	42.6 (2.1)	44.3 (2.0)	44.7 (2.3)	44.5 (2.4)	44.5 (2.5)	43.7 (3.3)	43.4 (3.7)	42.9 (3.9)
60-69	33.8 (4.2)	40.4 (3.7)	42.2 (4.0)	41.8 (4.3)	41.2 (4.8)	40.9 (4.9)	40.2 (4.9)	39.3 (5.9)	40.7 (4.3)
≥70	33.1 (3.6)	39.4 (2.6)	41.0 (2.7)	41.4 (3.0)	41.3 (3.7)	40.7 (3.7)	39.8 (4.5)	38.9 (5.2)	40.2 (3.0)
All 261 subjects	34.8 (3.9)	41.8 (2.9)	43.8 (2.9)	44.1 (3.3)	43.7 (3.7)	43.4 (3.9)	42.9 (4.3)	42.4 (4.8)	42.7 (3.2)

Last row demonstrates the average of all 261 subjects for a given annulus.

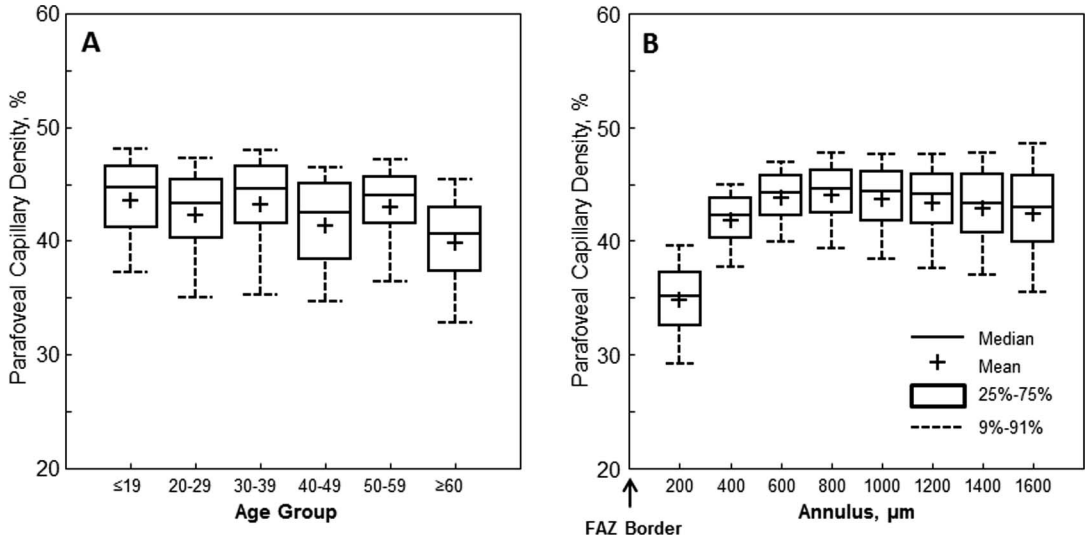

Figure 4. Boxplots show variation of parafoveal capillary density with (A) age group and (B) annular distance from the FAZ border. Parafoveal capillary density varied significantly with age group ($P = 3.5 \times 10^{-44}$) and annular distance ($P = 3.4 \times 10^{-176}$). No significant interaction between age group and annular distance was observed ($P = 0.592$).

varies across age groups in otherwise healthy individuals.[15–17,32] However, no significant correlation between parafoveal capillary density and age in years was detected after controlling for SSI (Table 2).When analyzing SSI in different age groups, the two oldest groups had significantly lower SSI compared to all other age groups, implying that decreased parafoveal capillary density with increasing age was possibly due to lower image quality in subjects older than 60 rather than aging (Sill AP, et al., *IOVS* 2017;58:ARVO E-Abstract 4749). Since lower OCT-A image quality due to reduced ocular media clarity in the older age group also would lead to reduced parafoveal capillary density values, caution should be applied when interpreting aging effect reported in prior studies without controlling for SSI.

The impact of aging on retinal vasculature has been an area of research and controversy for some time. Using IVFA and most recently OCT-A, researchers have sought to tease out the difference between normal aging and the changes associated with pathologic conditions.[15–17,31,32] Using OCT-A, while most studies found that vessel density decreased with age, two studies reported that age had no effect on vessel density.[33,34] The discrepancy in these results could be due to sample size, age range, image processing approach or confounding factors, such as use of both eyes from the same subject, inclusion of noncapillary blood vessels, lack of SSI control, or not accounting for axial length scaling.

Our results demonstrated that parafoveal capillary density increased with increasing annular distance from the FAZ border. The lowest capillary density was found at the innermost annulus adjacent to the FAZ border, where only a single layer of capillaries is present. This single-layer of capillaries is responsible for supplying nutrients to the outer border of the fovea, which is the most metabolically active region of the retina.[35] Since it is believed that homeostatic mechanisms gradually fail with aging, future studies should focus on evaluating microvascular changes with increasing retinal eccentricity from the fovea for better understanding of region-specific susceptibilities to aging.[36] In this study, we introduced a novel age-group and eccentricity matched deviation mapping technique to assess qualitatively and quantitatively the significance of parafoveal capillary density variations in individual eyes. The color-coding approach provides a simple and rapidly interpretable picture of the significance of deviations in parafoveal capillary density. This methodology has potential as a good screening tool in differentiating age-related changes from those of an early disease process and as a monitoring tool for detecting response to treatment. The clinical applicability of normative data-based deviation mapping extends into other parts of the retina, such as the peripapillary region as presented in previous studies from our lab. [37]

Our custom image processing methodology presents several advantages to previous approaches. Specifically, it takes into account individual FAZ variation and variation in capillary density with

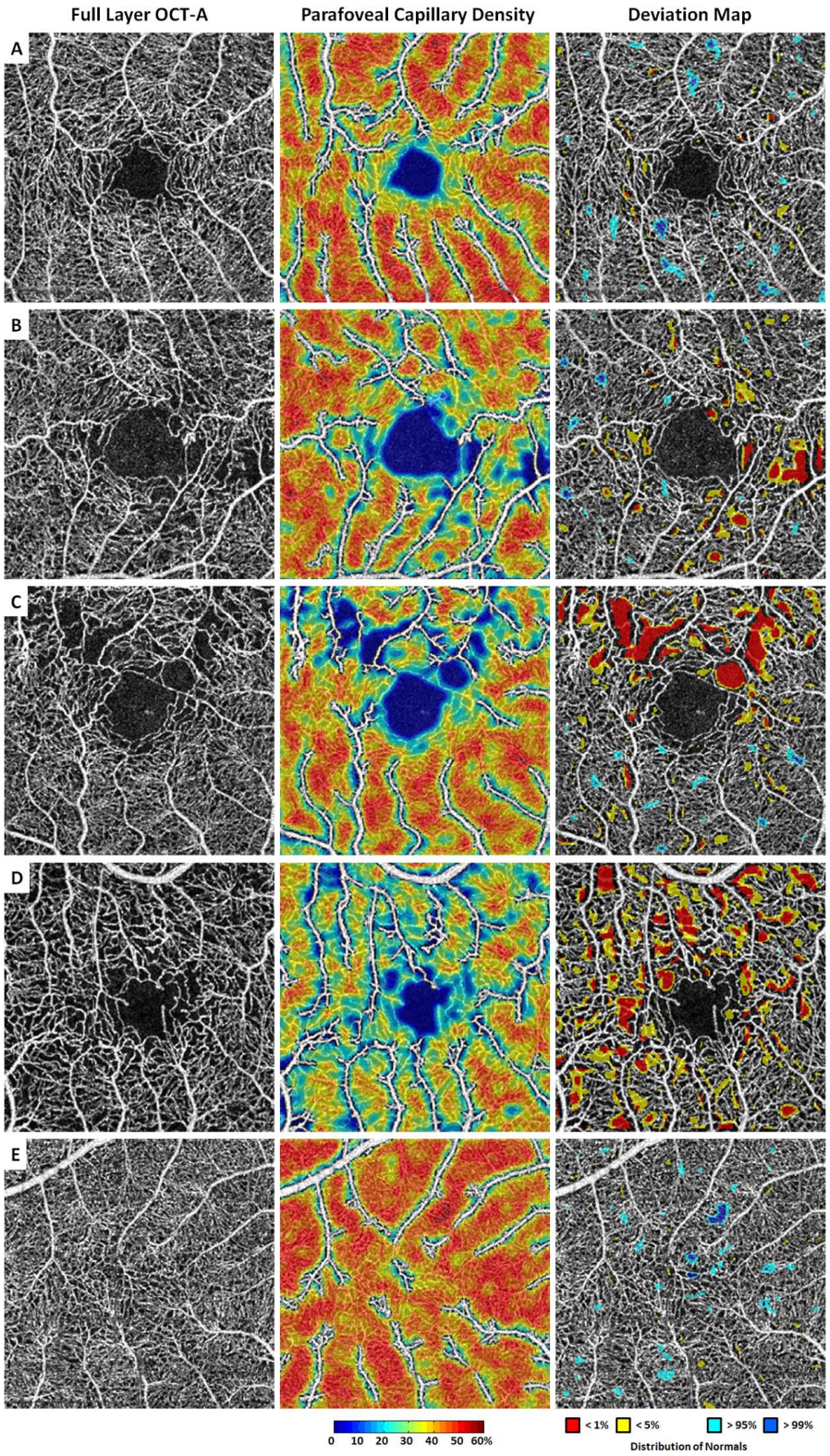

Figure 5. Comparison of parafoveal capillary density and deviation maps in healthy control and eyes with different retinal abnormalities. (A) Healthy control. (B) NPDR. (C) BRVO. (D) SCR. (E) Albinism. *Left column*: Contrast-stretched full layer OCT-A. *Middle column*: Parafoveal capillary density maps with noncapillary blood vessels indicated in white. *Right column*: On the deviation maps, whereas regions below 5% and 1% of the normative database are indicated in *yellow* and *red*, respectively; regions above 95% and 99% of the normative database are indicated in *cyan* and *blue*, respectively.

increasing eccentricity from the foveal center by excluding the area within the FAZ from analysis, and creating a series of equidistant annuli from the border of the FAZ. This allows standardization of ROIs among subjects. The other key aspect of our methodology was that we excluded noncapillary blood vessels from analysis. We are not the first group to do this. One other study removed noncapillary blood vessels from their capillary density analysis.[15] As mentioned in the introduction, noncapillary blood vessels have different anatomy and different lumen diameters compared to those of capillaries, and may be affected by physiologic and pathophysiologic processes differently.

Our methodology has several limitations. Study participants self-reported their past medical histories. To ensure a healthy retina, clinical fundus photographs and OCT scans of the macula and retinal nerve fiber layer surrounding the optic nerve head were obtained. No vital sign or laboratory testing was performed. An important limitation to the study was the relatively low number of individuals older than 70 years. Future studies should develop a larger normative database with evenly distributed sample size and wider age range that also control for sex- and race-related differences in vascular metrics as prior studies have shown sex- or race-bias in controls and disease eyes.[19,32,38,39] It is important to note that most previous studies did not correct for axial length magnification, as females have shorter eyes than males, the conclusions must be assessed carefully. Another limitation was that we used full layer scans containing the superficial and deep microvascular layers, and did not analyze them separately. This was performed to avoid the projection artifact of the superficial capillary layer onto the deeper capillary layers, which makes it difficult to study the deeper capillary layers separately. With the recent development of projection-resolved OCT-A,[40,41] future assessment and characterization of individual OCT-A vascular layers using our deviation mapping technique may further benefit diseases with layer-specific abnormalities. Newer studies using a 3D volumetric analysis of different ophthalmic structures, including the retinal vasculature, could prove to be the most accurate assessment yet.[42,43] The method in which our study generated deviation maps is another potential source of error. Since our normative database was constructed by measuring the parafoveal capillary density within multiple equidistant annuli around the FAZ margin, deviation maps generated with FAZ area outside the age group-specific normative range (Fig. 3A) should be interpreted with caution. Also, the demarcation of the FAZ border was performed on the OCT-A image, and not on the original structural FAZ that may contain nonperfused blood vessels at its true anatomic border. This source of error can potentially be solved by delineating the FAZ borders based on the respective en face reflectance OCT images. Since prior studies have shown that averaged en face reflectance images can be used to reveal the original FAZ border before disease onset,[44,45] generating the eight annuli and the subsequent deviation map based on this original FAZ border may, therefore, provide more accurate assessment of disease severity. This is especially important when analyzing eyes with retinopathy where the FAZ area is significantly larger than normal.[44] In addition, our deviation mapping approach was performed under the assumption that capillary density is evenly distributed around the FAZ in normal eyes, which may limit its sensitivity for detecting subtle deviation at the parafoveal region where nonuniform distribution of vessel density has been reported previously.[33,46]

In summary, we presented the effects of age, SSI, and retinal eccentricity on parafoveal capillary density in otherwise healthy individuals using a novel image processing methodology. An age-group– and eccentricity-matched normative database was created, and was used as the basis for a parafoveal capillary density deviation mapping technique, providing a simple and intuitive way to assess the status of parafoveal capillary density in individual eyes. We hope this approach of deviation mapping using a normative database will help clinicians and researchers in differentiating age-related changes from early subclinical disease.

Acknowledgments

Supported by the National Eye Institute of the National Institutes of Health (Bethesda, MD) under award numbers R01EY027301, R01EY024969, and P30EY001931. The content is solely the responsibility of the authors and does not necessarily represent the official views of the National Institutes of Health. Also supported by the New York Eye and Ear Infirmary Foundation Grant, Marrus Family Foundation, the Geraldine Violett Foundation, The Edward N. & Della L. Thome Memorial Foundation, and the Jorge N. Buxton Microsurgical Foundation.

The sponsors and funding organizations had no role in the design or conduct of this research.

Disclosure: **J.S. Andrade Romo**, None; **R.E. Linderman**, Optovue (C); **A. Pinhas**, None; **J. Carroll**, Optovue (F); **R.B. Rosen**, Opticology (I), Optovue (C), Astellas (C), Boehringer-Ingerheim (C), Nano-Retina (C), OD-OS (C), Regeneron (C), Diopsys (C), Guardion Health (C), Bayer (C), Genentech-Roche (C); **T.Y.P. Chui**, None

References

1. World Health Organization. *World Report on Aging and Health 2015*. Geneva, Switzerland: World Health Organization; 2015. Available at: https://www.who.int/ageing/events/world-report-2015-launch/en/
2. World Health Organization. *Global Health and Aging*. Bethesda, MD: US National Institute of Aging; 2011. Available at: https://www.who.int/ageing/publications/global_health.pdf?ua=1
3. Wittenborn JS, Zhang X, Feagan CW, et al. The economic burden of vision loss and eye disorders among the united states population younger than 40 years. *Ophthalmology*. 2013;120:1728–1735.
4. Romano AD, Serviddio G, de Matthaeis A, Bellanti F, Vendemiale G. Oxidative stress and aging. *J Nephrol*. 2010;23(suppl 15):S29–S36.
5. Wei YH, Lu CY, Lee HC, Pang CY, Ma YS. Oxidative damage and mutation to mitochondrial DNA and age-dependent decline of mitochondrial respiratory function. *Ann N Y Acad Sci*. 1998;854:155–170.
6. Wei YH, Lee HC. Oxidative stress, mitochondrial DNA mutation, and impairment of antioxidant enzymes in aging. *Exp Biol Med (Maywood)*. 2002;227:671–682.
7. Catita J, Lopez-Luppo M, Ramos D, et al. Imaging of cellular aging in human retinal blood vessels. *Exp Eye Res*. 2015;135:14–25.
8. Salvi SM, Akhtar S, Currie Z. Ageing changes in the eye. *Postgrad Med J*. 2006;82:581–587.
9. Kennedy CJ, Rakoczy PE, Constable IJ. Lipofuscin of the retinal pigment epithelium: a review. *Eye (Lond)*. 1995;9:763–771.
10. Friedman DS, O'colmain B, Mestril I. *Vision Problems in the U.S*. Washington DC: Prevent Blindness America; 2012.
11. Flammer J, Konieczka K, Bruno RM, Virdis A, Flammer AJ, Taddei S. The eye and the heart. *Eur Heart J*. 2013;34:1270–1278.
12. Yu DY, Cringle SJ. Oxygen distribution and consumption within the retina in vascularised and avascular retinas and in animal models of retinal disease. *Prog Retin Eye Res*. 2001;20:175–208.
13. Nag TC, Wadhwa S. Ultrastructure of the human retina in aging and various pathological states. *Micron*. 2012;43:759–781.
14. Grossniklaus HE, Nickerson JM, Edelhauser HF, Bergman LA, Berglin L. Anatomic alterations in aging and age-related diseases of the eye. *Invest Ophthalmol Vis Sci*. 2013;54:ORSF23–27.
15. Wei Y, Jiang H, Shi Y, et al. Age-related alterations in the retinal microvasculature, microcirculation, and microstructure. *Invest Ophthalmol Vis Sci*. 2017;58:3804–3817.
16. Yu J, Jiang C, Wang X, et al. Macular perfusion in healthy chinese: an optical coherence tomography angiogram study. *Invest Ophthalmol Vis Sci*. 2015;56:3212–3217.
17. Garrity ST, Iafe NA, Phasukkijwatana N, Chen X, Sarraf D. Quantitative analysis of three distinct retinal capillary plexuses in healthy eyes using optical coherence tomography angiography. *Invest Ophthalmol Vis Sci*. 2017;58:5548–5555.
18. Samara WA, Say EA, Khoo CT, et al. Correlation of foveal avascular zone size with foveal morphology in normal eyes using optical coherence tomography angiography. *Retina*. 2015;35:2188–2195.
19. Linderman R, Salmon AE, Strampe M, Russillo M, Khan J, Carroll J. Assessing the accuracy of foveal avascular zone measurements using optical coherence tomography angiography: segmentation and scaling. *Transl Vis Sci Technol*. 2017;6:16.
20. Chylack LT Jr, Wolfe JK, Singer DM, et al. The lens opacities classification system III. the longitudinal study of cataract study group. *Arch Ophthalmol*. 1993;111:831–836.
21. Bunce C, Quartilho A, Freemantle N, Dore CJ, Ophthalmic Statistics G. Ophthalmic statistics note 8: missing data–exploring the unknown. *Br J Ophthalmol*. 2016;100:291–294.
22. Jia Y, Tan O, Tokayer J, et al. Split-spectrum amplitude-decorrelation angiography with optical coherence tomography. *Opt Express*. 2012;20:4710–4725.
23. Freiberg FJ, Pfau M, Wons J, Wirth MA, Becker MD, Michels S. Optical coherence tomography angiography of the foveal avascular zone in diabetic retinopathy. *Graefes Arch Clin Exp Ophthalmol*. 2016;254:1051–1058.
24. Sampson DM, Gong P, An D, et al. Axial length variation impacts on superficial retinal vessel

density and foveal avascular zone area measurements using optical coherence tomography angiography. *Invest Ophthalmol Vis Sci*. 2017;58:3065–3072.
25. Krawitz BD, Mo S, Geyman LS, et al. Acircularity index and axis ratio of the foveal avascular zone in diabetic eyes and healthy controls measured by optical coherence tomography angiography. *Vision Res*. 2017;139:177–186.
26. Iafe NA, Phasukkijwatana N, Chen X, Sarraf D. Retinal capillary density and foveal avascular zone area are age-dependent: quantitative analysis using optical coherence tomography angiography. *Invest Ophthalmol Vis Sci*. 2016;57:5780–5787.
27. Wu LZ, Huang ZS, Wu DZ, Chan E. Characteristics of the capillary-free zone in the normal human macula. *Jpn J Ophthalmol*. 1985;29:406–411.
28. Bird AC, Weale RA. On the retinal vasculature of the human fovea. *Exp Eye Res*. 1974;19:409–417.
29. Chui TY, VanNasdale DA, Elsner AE, Burns SA. The association between the foveal avascular zone and retinal thickness. *Invest Ophthalmol Vis Sci*. 2014;55:6870–6877.
30. Chui TY, Zhong Z, Song H, Burns SA. Foveal avascular zone and its relationship to foveal pit shape. *Optom Vis Sci*. 2012;89:602–610.
31. Laatikainen L, Larinkari J. Capillary-free area of the fovea with advancing age. *Invest Ophthalmol Vis Sci*. 1977;16:1154–1157.
32. Coscas F, Sellam A, Glacet-Bernard A, et al. Normative data for vascular density in superficial and deep capillary plexuses of healthy adults assessed by optical coherence tomography angiography. *Invest Ophthalmol Vis Sci*. 2016;57:OCT211–223.
33. Gadde SG, Anegondi N, Bhanushali D, et al. Quantification of vessel density in retinal optical coherence tomography angiography images using local fractal dimension. *Invest Ophthalmol Vis Sci*. 2016;57:246–252.
34. Yu J, Gu R, Zong Y, et al. Relationship between retinal perfusion and retinal thickness in healthy subjects: an optical coherence tomography angiography study. *Invest Ophthalmol Vis Sci*. 2016;57:OCT204–210.
35. Wong-Riley MT. Energy metabolism of the visual system. *Eye Brain*. 2010;2:99–116.
36. Velez G, Machlab DA, Tang PH, et al. Proteomic analysis of the human retina reveals region-specific susceptibilities to metabolic- and oxidative stress-related diseases. *PLoS One*. 2018;13:e0193250.
37. Pinhas A, Linderman R, Mo S, et al. A method for age-matched oct angiography deviation mapping in the assessment of disease- related changes to the radial peripapillary capillaries. *PLoS One*. 2018;13:e0197062.
38. Weatherall DJ, Clegg JB. Inherited haemoglobin disorders: an increasing global health problem. *Bull World Health Organ*. 2001;79:704–712.
39. Rogers S, McIntosh RL, Cheung N, et al. The prevalence of retinal vein occlusion: pooled data from population studies from the United States, Europe, Asia, and Australia. *Ophthalmology*. 2010;117:313–319 e311.
40. Zhang M, Hwang TS, Campbell JP, et al. Projection-resolved optical coherence tomographic angiography. *Biomed Opt Express*. 2016;7:816–828.
41. Zhang M, Hwang TS, Dongye C, Wilson DJ, Huang D, Jia Y. Automated quantification of nonperfusion in three retinal plexuses using projection-resolved optical coherence tomography angiography in diabetic retinopathy. *Invest Ophthalmol Vis Sci*. 2016;57:5101–5106.
42. Kim DY, Fingler J, Werner JS, Schwartz DM, Fraser SE, Zawadzki RJ. In vivo volumetric imaging of human retinal circulation with phase-variance optical coherence tomography. *Biomed Opt Express*. 2011;2:1504–1513.
43. Poddar R, Zawadzki RJ, Cortés DE, Mannis MJ, Werner JS. In vivo volumetric depth-resolved vasculature imaging of human limbus and sclera with 1μm swept source phase-variance optical coherence angiography. *J Opt*. 2015;17:065301.
44. Lynch G, Andrade Romo JS, Linderman R, et al. Within-subject assessment of foveal avascular zone enlargement in different stages of diabetic retinopathy using en face oct reflectance and oct angiography. *Biomed Opt Express* 2018;9:5982.
45. Krawitz BD, Phillips E, Bavier RD, et al. Parafoveal nonperfusion analysis in diabetic retinopathy using optical coherence tomography angiography. *Transl Vis Sci Technol*. 2018;7:4.
46. Pinhas A, Razeen M, Dubow M, et al. Assessment of perfused foveal microvascular density and identification of nonperfused capillaries in healthy and vasculopathic eyes. *Invest Ophthalmol Vis Sci*. 2014;55:8056–8066.